Original Article

Dominant-Negative Effects of a Novel Mutated *Ins2* Allele Causes Early-Onset Diabetes and Severe β-Cell Loss in Munich *Ins2*^{C95S} Mutant Mice

Nadja Herbach,[1] Birgit Rathkolb,[2] Elisabeth Kemter,[1] Lisa Pichl,[1] Matthias Klaften,[3] Martin Hrabé de Angelis,[3] Philippe A. Halban,[4] Eckhard Wolf,[2] Bernhard Aigner,[2] and Ruediger Wanke[1]

The novel diabetic mouse model Munich *Ins2*^{C95S} was discovered within the Munich *N*-ethyl-*N*-nitrosourea mouse mutagenesis screen. These mice exhibit a T→A transversion in the insulin 2 (*Ins2*) gene at nucleotide position 1903 in exon 3, which leads to the amino acid exchange C95S and loss of the A6-A11 intrachain disulfide bond. From 1 month of age onwards, blood glucose levels of heterozygous Munich *Ins2*^{C95S} mutant mice were significantly increased compared with controls. The fasted and postprandial serum insulin levels of the heterozygous mutants were indistinguishable from those of wild-type littermates. However, serum insulin levels after glucose challenge, pancreatic insulin content, and homeostasis model assessment (HOMA) β-cell indices of heterozygous mutants were significantly lower than those of wild-type littermates. The initial blood glucose decrease during an insulin tolerance test was lower and HOMA insulin resistance indices were significantly higher in mutant mice, indicating the development of insulin resistance in mutant mice. The total islet volume, the volume density of β-cells in the islets, and the total β-cell volume of heterozygous male mutants was significantly reduced compared with wild-type mice. Electron microscopy of the β-cells of male mutants showed virtually no secretory insulin granules, the endoplasmic reticulum was severely enlarged, and mitochondria appeared swollen. Thus, Munich *Ins2*^{C95S} mutant mice are considered a valuable model to study the mechanisms of β-cell dysfunction and death during the development of diabetes. *Diabetes* 56:1268–1276, 2007

From the [1]Institute of Veterinary Pathology, University of Munich, Munich, Germany; the [2]Institute of Molecular Animal Breeding/Gene Center, University of Munich, Munich, Germany; the [3]Institute of Experimental Genetics, GSF-National Research Center for Environment and Health, Neuherberg, Germany; and the [4]Department of Genetic Medicine and Development, CMU, Geneva, Switzerland.

Address correspondence and reprint requests to Nadja Herbach, Institute of Veterinary Pathology, Veterinaerstr. 13, 80539 Munich, Germany. E-mail: herbach@patho.vetmed.uni-muenchen.de.

Received for publication 12 May 2006 and accepted in revised form 6 February 2007.

Published ahead of print at http://diabetes.diabetesjournals.org on 15 February 2007. DOI: 10.2337/db06-0658.

ENU, *N*-ethyl-*N*-nitrosourea; HOMA, homeostasis model assessment; OGTT, oral glucose tolerance test; PP, pancreatic polypeptide.

The prevalence of diabetes has reached an alarming dimension in industrialized countries and turned into a major health concern. More than 170 million people suffer from diabetes worldwide, and this number is expected to rise substantially within the next decades (1). Despite its high prevalence, the pathogenesis of diabetes is still not completely understood. Appropriate experimental models are essential tools to get more insight into the genetics and pathogenesis of this multifaceted disease.

N-ethyl-*N*-nitrosourea (ENU) has been used in various mouse mutagenesis programs for the production of random mutations. In this study, we present the genotypic and phenotypic findings of the novel nonobese diabetic mouse model Munich *Ins2*^{C95S}, which was found in the screen for dominant mutations in the Munich ENU mouse mutagenesis project.

RESEARCH DESIGN AND METHODS

Animals and breeding design. The Munich ENU mouse mutagenesis project was carried out on the inbred C3HeB/FeJ (C3H) genetic background as described (2). Standard rodent diet (Altromin, Lage, Germany) and water were provided ad libitum. All animal experiments were carried out under the approval of the responsible animal welfare authority.

Linkage analysis of the mutation. For linkage analysis, male heterozygous diabetic C3HeB/FeJ mutants were mated to C57BL/6Jico (C57BL/6) female mice (Charles River, Sulzfeld, Germany). The resulting diabetic F1 hybrid males were backcrossed to C57BL/6 females. After euthanization, tissue samples of 92 diabetic and nondiabetic N2 mice were collected for subsequent DNA isolation.

Tail clip samples were incubated over night with a lysis buffer as described elsewhere (3) and 300 μg/ml Proteinase K (Sigma-Aldrich, Taufkirchen, Germany). Automated DNA extraction from the lysates was performed using the AGOWA Mag Maxi DNA Isolation kit (AGOWA, Berlin, Germany). For linkage analysis, genotyping of a genome-wide mapping panel consisting of 149 single nucleotide polymorphisms was performed using MassExtend, a MALDI-TOF (matrix-assisted laser/desorption ionization, time of flight analyzer) mass spectometry high-throughput genotyping system supplied by Sequenom (San Diego, CA).

Candidate gene analysis of *Ins2*. For cDNA sequence analysis of the candidate gene *Ins2*, total RNA was isolated from the pancreas of heterozygous mutant mice, using the RNeasy Mini kit (Qiagen, Hilden, Germany). After DNase I digestion, reverse transcription was carried out as previously described (4) using oligo (dT) primers, and RT-PCR was performed using the primer pair Ins2_1se (nt 958–977) and Ins2_1as (nt 1964–1944) (GenBank accession no. X04724). RT-PCR products (417 bp) were purified using the QIAquick Gel Extraction kit (Qiagen) and sequenced bidirectionally.

In addition, *Ins2* was sequenced on the genomic DNA level. DNA from homozygous mutants and wild-type mice was extracted from tail tips using the Wizard genomic DNA purification kit (Promega, Madison, WI) and amplified

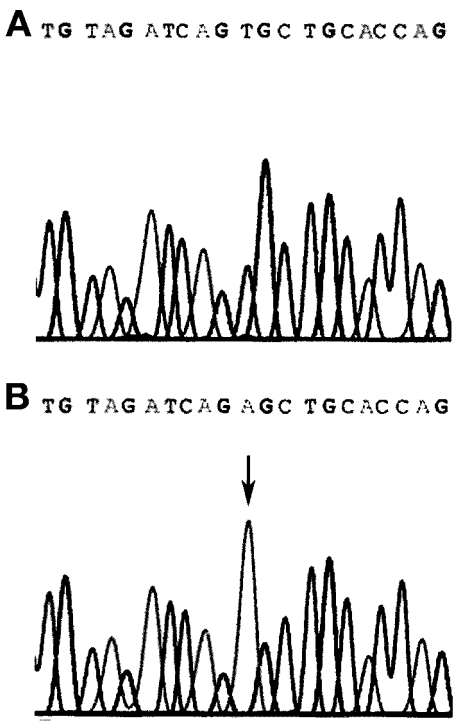

FIG. 1. Sequence of the *Ins2* gene of a wild-type (*A*) and a Munich *Ins2*^{C95S} mutant (*B*) mouse. The point mutation at nucleotide position 1903 is marked with an arrow.

using the primer pairs Ins2_1se and Ins2_1as, Ins2_2se (nt 103–123) and Ins2_2as (nt 12831–264), and Ins2_3se (nt 18451–864) and Ins2_3as (nt 23732–354). The sequences were aligned to the mouse preproinsulin gene II (GenBank accession no. X04724). For the allelic differentiation of *Ins2*, mutant animals were identified using a restriction fragment–length polymorphism–based strategy. The primers Ins2_3se and Ins2_3as resulted in 529-bp PCR products, which were restricted by the enzyme *Hpy* 188I (New England Biolabs, Frankfurt, Germany).

Body weights. The fasting body weight of 1-, 3-, and 6-month-old heterozygous mutant and wild-type mice was determined to the nearest 0.1 g. The body weight of randomly fed homozygous mutant and wild-type mice was determined at 4 weeks of age.

Glucose and insulin analyses. For phenotyping of N2 progeny, blood glucose of randomly fed animals was measured at 4 and 8 weeks of age, using the Super GLeasy system (Dr. Müller Gerätebau, Freital, Germany). Blood glucose of heterozygous mutant and wild-type animals on C3H genetic background was determined at 3 weeks of age in randomly fed mice (10:00 A.M.) and at 1 and 3 months of age after 1.5 h refeeding, following a 15-h fasting period (7:00 P.M. to 10:00 A.M.). Blood glucose of homozygous mutant and wild-type mice was determined in randomly fed animals at 3 weeks of age.

Oral glucose tolerance tests (OGTTs) were performed after a 15-h fasting period (7:00 P.M. to 10:00 A.M.) at 1, 3, and 6 months of age. Via gavage tube, 11.1 μl 1 mol/l glucose solution was administered per gram of body weight. Blood glucose concentrations were determined at the indicated time points.

Serum insulin concentration was measured in fasted mice, 10 min after glucose challenge, and after 1.5-h refeeding at 1, 3, and 6 months of age as previously described (5).

The homeostasis model assessment (HOMA) of β-cell function index and HOMA of insulin resistance index was calculated as described previously (6).

Insulin tolerance tests were performed in 4-month-old male animals. Insulin (1 unit/kg body wt) (Huminsulin; Lilly, Giessen, Germany) was administered intraperitoneally, and blood glucose levels were measured at the indicated time points.

Pancreatic insulin content of 3- and 6-month-old heterozygous mutant and wild-type mice was determined as described (7). Protein content was determined photometrically; insulin concentration was analyzed by radioimmunoassay (Linco Research).

Pancreas preparation and morphometric analysis. The morphologic changes of the endocrine pancreas of 6-month-old heterozygous Munich *Ins2*^{C95S} mutant mice were quantitatively evaluated using unbiased model-independent stereological methods (8,9) as described (5). Briefly, the volume density of islets in the pancreas [$Vv_{(Islet/Pan)}$] was calculated dividing the sum of cross-sectional areas (ΣA) of islets by ΣA pancreas. The total islet volume [$V_{(Islet,\ Pan)}$] was calculated by multiplying $Vv_{(Islet/Pan)}$ and $V_{(Pan)}$. Volume densities of different endocrine cells in the islets [$Vv_{(X\text{-}cells/Islet)}$] were determined by dividing ΣA of α-, δ-, and pancreatic polypeptide (PP)-cells, respectively, by ΣA islets. The total volume of endocrine cells [$V_{(X\text{-}cells,\ Islet)}$] was obtained by multiplying $Vv_{(X\text{-}cells/Islet)}$ and $V_{(Islet,\ Pan)}$. β-Cells of mutant mice weakly stained positive for insulin due to severe degranulation; hence, measurement of ΣA β-cells led to an underestimation of $Vv_{(B\text{-}cells/Islet)}$ and $V_{(B\text{-}cells,\ Islet)}$. Therefore, $V_{(B\text{-}cells,\ Islet)}$ was calculated by subtracting $V_{(Non\text{–}B\text{-}cells,\ Islet)}$ from $V_{(Islet,\ Pan)}$. Then, $Vv_{(B\text{-}cells/Islet)}$ was calculated by dividing $V_{(B\text{-}cells,\ Islet)}$ by $V_{(Islet,\ Pan)}$.

Immunohistochemistry. The indirect immunoperoxidase method was used to determine insulin-, glucagon-, somatostatin-, and PP-containing cells as previously described (5). Horseradish-conjugated rabbit anti–guinea pig IgG and pig anti-rabbit IgG were from Dako Diagnostika (Hamburg, Germany).

Electron microscopy. Pancreas samples were fixed in 6.25% glutaraldehyde in Sorensen's phosphate buffer (pH 7.4) for 24 h. Six to eight 1-mm^3 samples were postfixed in 1% osmium tetroxid and routinely embedded in Epon. Ultrathin sections (70–80 nm) were stained with uranyl citrate and lead citrate and examined with an EM10 transmission electron microscope (Zeiss, Oberkochen, Germany).

Data presentation and statistical analysis. Data are presented as means ± SE or SD as indicated. The general linear models procedure was used in order to calculate least-squares means; comparison of the least-squares means of different groups was performed using the Student's *t* test (SAS release 8.2; SAS Institute, Heidelberg, Germany). *P* values <0.05 were considered significant.

RESULTS

Establishment of the hyperglycemic line. In the screen for dominant mutations of the Munich ENU mouse mutagenesis project, a male G_1 offspring (no. 20016135) of an ENU-treated C3H mouse showed hyperglycemia (276 and 335 mg/dl, respectively) in two subsequent examinations at 12 and 15 weeks of age. Mating of the hyperglycemic G_1 mouse to a wild-type C3H female resulted in the inheritance of the abnormal phenotype to the G_2 offspring, which revealed an autosomal dominant mutation as cause for the aberrant phenotype. Subsequently, a mutant line (GLS004) was established by breeding heterozygous mutants to wild-type mice of the C3H genetic background for >10 generations.

Linkage analysis and candidate gene examination of *Ins2*. The genome-wide linkage analysis revealed a strong linkage ($\chi^2 = 76.6$; $P < 0.0001$) of the mutation to a defined single chromosomal site on chromosome 7, represented by the marker rs13479566 at 136.88 Mb (mouse genome build 35.1).

The sequence analysis of the positional candidate gene *Ins2* consistently revealed a T→A transversion at nucleotide position 1903 in exon 3 (GenBank accession no. X04724) (Fig. 1). The mutation leads to an amino acid exchange from cysteine to serine at position 95, corresponding to amino acid 6 on the A chain (A6), which forms the intrachain disulfide bond with cysteine100 (A11). The replacement of C95 therefore leads to the loss of the A6-A11 intrachain disulfide bond. According to the mutation, the diabetic strain was named Munich *Ins2*^{C95S}.

The missense mutation found in exon 3 of *Ins2* creates a new *Hpy* 188I restriction site that was used for the allelic differentiation of *Ins2*. Digested 529-bp PCR amplificates of wild-type mice showed a 521-bp fragment, heterozygous Munich *Ins2*^{C95S} mutant mice showed both the 473- and 521-bp fragment (Fig. 2), and homozygous mutants demonstrated the 473-bp fragment (data not shown).

Phenotyping of N2 progeny. Animals showing glucosuria or exhibiting blood glucose levels >160 mg/dl for females and 190 mg/dl for males were considered diabetic. A total of 290 N2 progeny (146 males and 144 females) were investigated. Forty-eight percent of the male and 41%

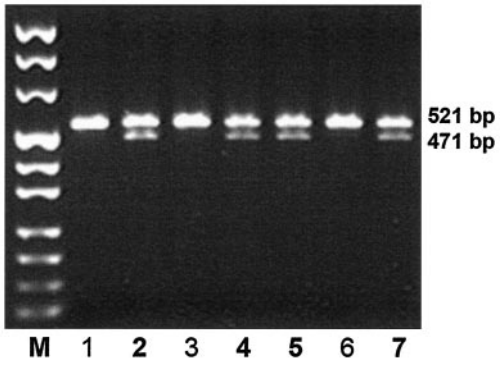

FIG. 2. PCR result. M, marker (MBI Fermentas, St. Leon-Rot, Germany); bold numbers represent heterozygous Munich *Ins2*^{C95S} mutant mice.

of the female mice showed a diabetic phenotype (70 males and 59 females). Ten percent of the females and 3% of the males investigated showed an uncertain diabetic phenotype, and 49% of both males and females were considered nondiabetic. Therefore, the examination of the diabetic phenotype showed complete phenotypic penetrance of the autosomal dominant mutation according to the sign test after Dixon and Mood (5 and 1% level) (10).

Body weights. At 1 month of age, fasted body weights of heterozygous mutant and wild-type mice were similar (data not shown). The fasted body weights of 3- and 6-month-old male heterozygous Munich *Ins2*^{C95S} mutant mice were significantly lower than that of sex-matched littermate controls (Table 1).

Glucose and insulin analyses. At 3 weeks of age, blood glucose levels did not differ between heterozygous mutant and wild-type mice. At 1, 3, and 6 months of age, fasted and 1.5-h postprandial blood glucose levels were significantly elevated in both male ($n = 5$) and female ($n = 5$) Munich

TABLE 1
Body weights

Group	Body weight (g)	
	3 months	6 months
Male, wild type (4/5)	26.7 ± 1.9	29.5 ± 3.8
Male, mutant (4/5)	23.5 ± 1.4*	22.8 ± 1.6*
Female, wild type (4/5)	23.3 ± 1.3	26.1 ± 5.5
Female, mutant (4/5)	23.0 ± 0.7	25.0 ± 1.7

Data are means ± SD. (4/5), number of animals examined at 3 and 6 months of age. *$P < 0.05$.

Ins2^{C95S} mutant mice compared with age- and sex-matched wild-type mice. One-month-old females, as well as 3- and 6-month-old male and female mutants, showed significantly elevated blood glucose levels at all time points during the OGTT; in 1-month-old males, blood glucose was elevated in the fasted state and from 20 min onwards during the OGTT (Fig. 3).

Postprandial and 20- to 90-min OGTT blood glucose levels of 1-month-old male Munich *Ins2*^{C95S} mutant mice were significantly higher than those of female mutant mice ($P < 0.05$). At 3 and 6 months of age, blood glucose levels of male mutants were always significantly higher than those of females ($P < 0.001$).

Fasted blood glucose levels deteriorated significantly from 1 to 3 and from 3 to 6 months in male mutants. The fasted and 1.5-h postprandial immunoreactive serum insulin levels of male and female Munich *Ins2*^{C95S} mutant mice did not differ from those of sex-matched controls (data not shown). At 10 min after glucose challenge, the serum insulin levels of both male and female mutants were significantly reduced compared with controls, irrespective of the age at sampling (Fig. 4*A*). The HOMA β-cell index was determined at 1, 3, and 6 months of age and found to be largely reduced at any age investigated (Fig. 4*B*).

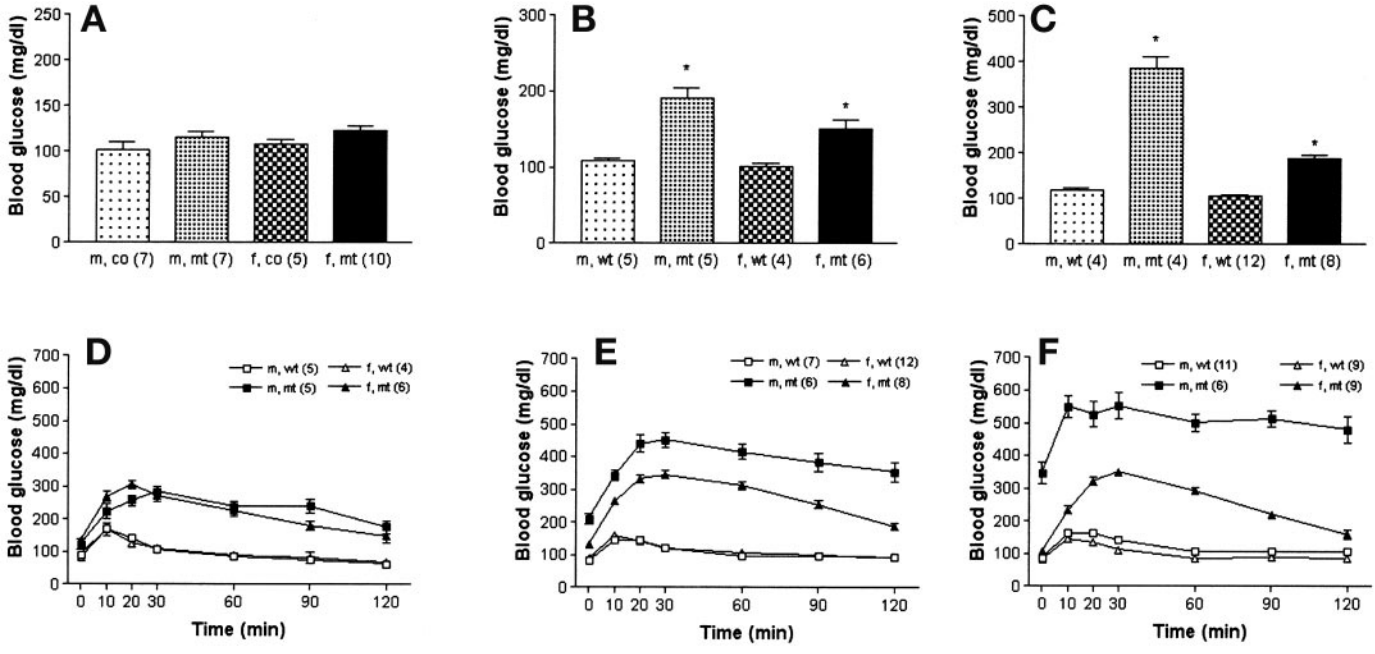

FIG. 3. Postprandial blood glucose levels (*A–C*) and OGTT (*D–F*) at 3 weeks (*A*) and 1 (*B* and *D*), 3 (*C* and *E*), and 6 (*F*) months of age. Blood glucose levels from randomly fed mutant (mt) mice at 3 weeks of age do not differ from those of controls. Postprandial blood glucose levels of Munich *Ins2*^{C95S} mutant mice at 1 and 3 months of age are significantly higher than those of wild-type (wt) mice. The fasted blood glucose and glucose levels during an OGTT are significantly higher in Munich *Ins2*^{C95S} mutant mice compared with wild-type mice. Data represent means and SE. *$P < 0.05$. f, female; m, male.

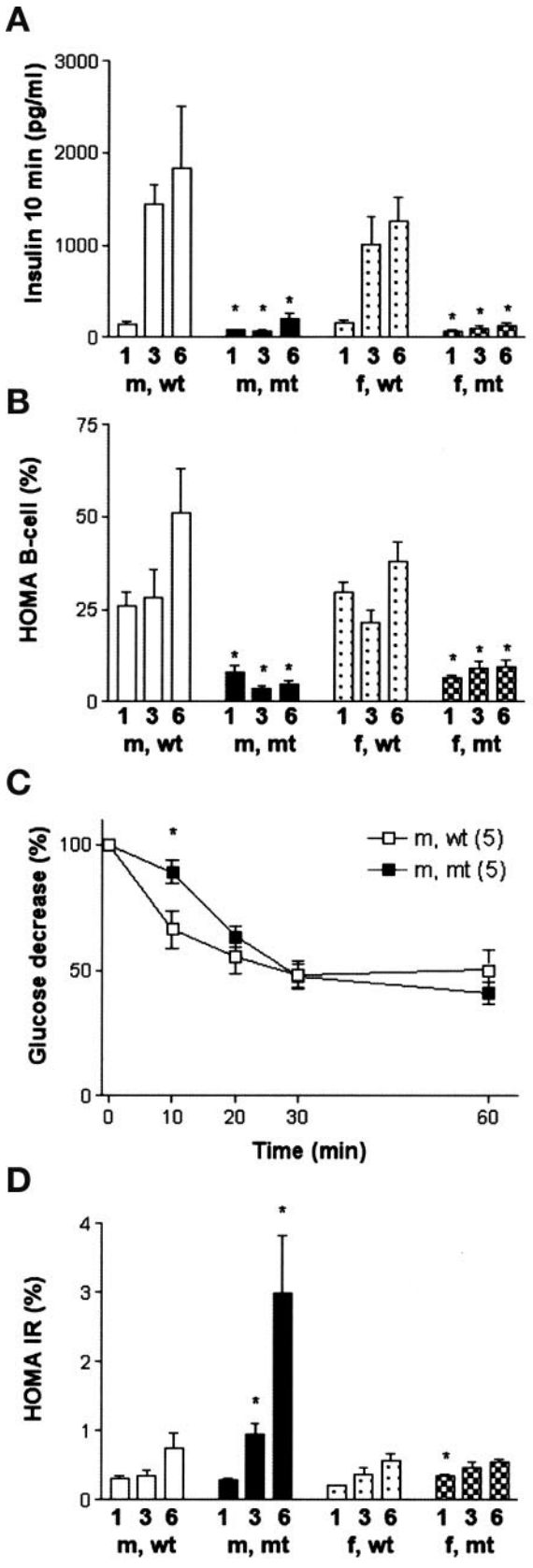

FIG. 4. Serum insulin levels 10 min after glucose challenge (*A*), HOMA of β-cell index (*B*), insulin tolerance test (*C*), and HOMA of insulin resistance (IR) index (*D*) at 1, 3, and 6 months of age. Serum insulin levels (*A*) and HOMA of β-cell indices (*B*) of Munich *Ins2*^{C95S} mutant (mt) mice are significantly lower than those of wild-type (wt) mice. *C*: Blood glucose decrease from basal is significantly less in mutants versus wild-type mice. *D*: One-month-old female (f) mutants and 3- and 6-month-old male (m) mutants show significantly higher HOMA of insulin resistance indices than wild-type mice. Data represent means and SE. *$P < 0.05$.

Insulin tolerance tests were performed in 4-month-old male mice. The decrease in blood glucose levels from basal to 10 min after insulin injection was significantly smaller in Munich *Ins2*^{C95S} mutants than in wild-type mice. The further decrease of blood glucose was nearly identical in mutants and wild-type mice (Fig. 4*C*). The HOMA of insulin resistance was significantly higher in 1-month-old female mutants and in 3- and 6-month-old male mutants (Fig. 4*D*). Pancreatic insulin content was significantly reduced in both male and female Munich *Ins2*^{C95S} mutant mice, irrespective of the age at sampling (Fig. 5).

Homozygous mutant mice. Homozygous mutant mice were born at the expected Mendelian frequency and developed normally until 18 days of age. As evidenced by glucosuria, diabetes occurred at this time point. At 21 days of age, blood glucose levels were largely increased in both male ($n = 14$) and female ($n = 9$) mutants compared with wild-type mice (male 400 ± 123 vs. 111 ± 17 mg/dl and female 394 ± 150 vs. 107 ± 6 mg/dl). The body weight of homozygous mutants was significantly reduced at 28 days of age compared with wild-type mice (male 11 ± 2 vs. 17 ± 2 g and female 10 ± 4 vs. 15 ± 2 g). Homozygous male ($n = 14$) and female ($n = 9$) mutants died at a mean age of 46 days (range 31–76) and 52 days (33–75), weighing 9 ± 2 and 7 ± 1 g, respectively.

Immunohistochemical and quantitative stereological investigations of the endocrine pancreas. At 6 months of age, the pancreas volume (V_{pan}) (Fig. 6*A*), as well as gross morphology and histologic appearance of the exocrine pancreas, were unchanged in Munich *Ins2*^{C95S} mutant mice, and no signs of insulitis were observed. Immunohistochemistry for insulin and glucagon revealed an atypical composition and organization of islets of Munich *Ins2*^{C95S} mutants. Very few islet cells stained insulin positive, and the staining intensity was very weak, whereas the proportion of cells expressing glucagon was increased. α-Cells were dispersed over the islet profile in mutant mice, which was markedly different from the typical distribution of endocrine cells in murine pancreatic islets, being characterized by a ring of non–β-cells surrounding a core of β-cells (Fig. 5*A–D*).

The total islet volume of Munich *Ins2*^{C95S} mutant male mice was significantly lower than that of wild-type mice (Fig. 6*B*). Due to the weak insulin-staining intensity of β-cells, the measurement of the insulin-positive area resulted in an underestimation of the total β-cell volume and the volume density of β-cells in the islets (data not shown). Therefore, the total β-cell volume was calculated by subtracting the total volumes of α-, δ-, and PP-cells from the total islet volume. The calculated total β-cell volume was decreased by 81% in Munich *Ins2*^{C95S} mutant males ($P < 0.001$) and by 19% in females (P = NS) compared with sex-matched wild-type mice (Fig. 6*D*). The calculated volume density of β-cells of mutant males was also significantly lower compared with male wild-type mice; the difference in the total β-cell volume and the volume density of β-cells in the islets of female mutants versus wild-type mice did not reach statistical significance (Fig. 6*C*).

Volume densities of α-, δ-, and PP-cells in the islets, as well as the total volumes of δ- and PP-cells, were signifi-

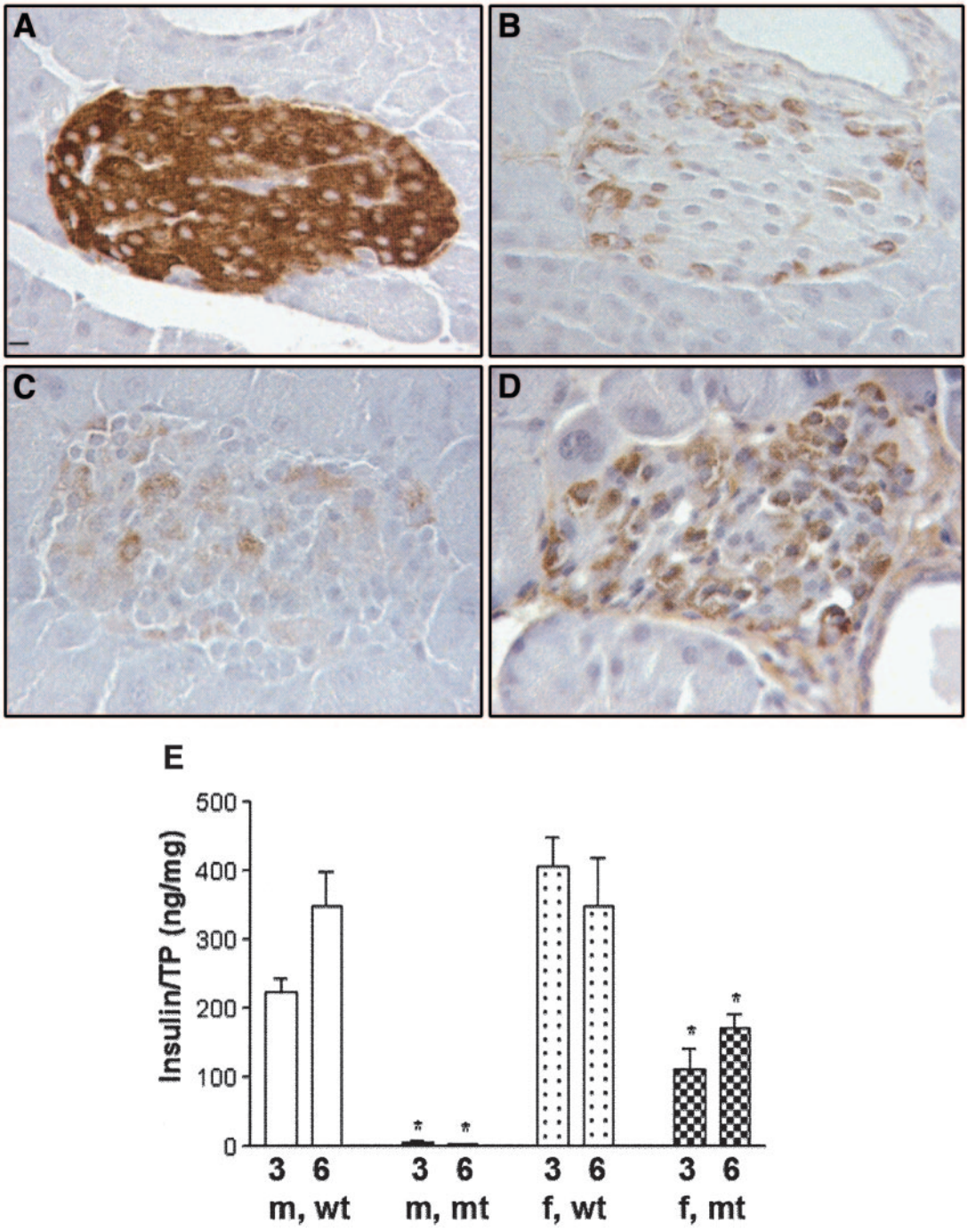

FIG. 5. Distribution of β- (*A* and *C*) and α- (*B* and *D*) cells in islets of wild-type (*A* and *B*) and Munich *Ins2*^{C95S} mutant mice (*C* and *D*) and pancreatic insulin content (*E*). The proportion of insulin-producing cells is severely reduced and the staining intensity for insulin is weak in mutant mice. The proportion of α-cells is increased and α-cells are dispersed over the islet profile in mutant mice. *E*: The insulin content in the pancreas is significantly lower than that of wild-type mice. Data represent means and SE. **P* < 0.05.

cantly higher in male Munich *Ins2*^{C95S} mutants compared with wild-type males (Fig. 6*E* and *G–J*). Both the volume density of α-cells in the islets and the total α-cell volume of mutant females were significantly higher compared with wild-type females (Fig. 6*E* and *F*).

Electron microscopy. Electron microscopy revealed a variety of ultrastructural changes of the β-cells of heterozygous Munich *Ins2*^{C95S} mutant mice, including prominent disorganization of the rough endoplasmic reticulum, appearing as dilated cisternae, as well as mitochondrial swelling with largely destroyed crests and apparent myelin figures. The insulin secretory granules were almost missing, and remaining granules appeared small with electron lucent or dense cores and only a thin or no halo between the content and the limiting membrane (Fig. 7). β-Cells exhibited vacuolization, but neither apoptotic bodies nor chromatin condensation were observed in the damaged β-cells of Munich *Ins2*^{C95S} mutant mice. The Golgi apparatus of β-cells showed no obvious changes compared with wild-type mice.

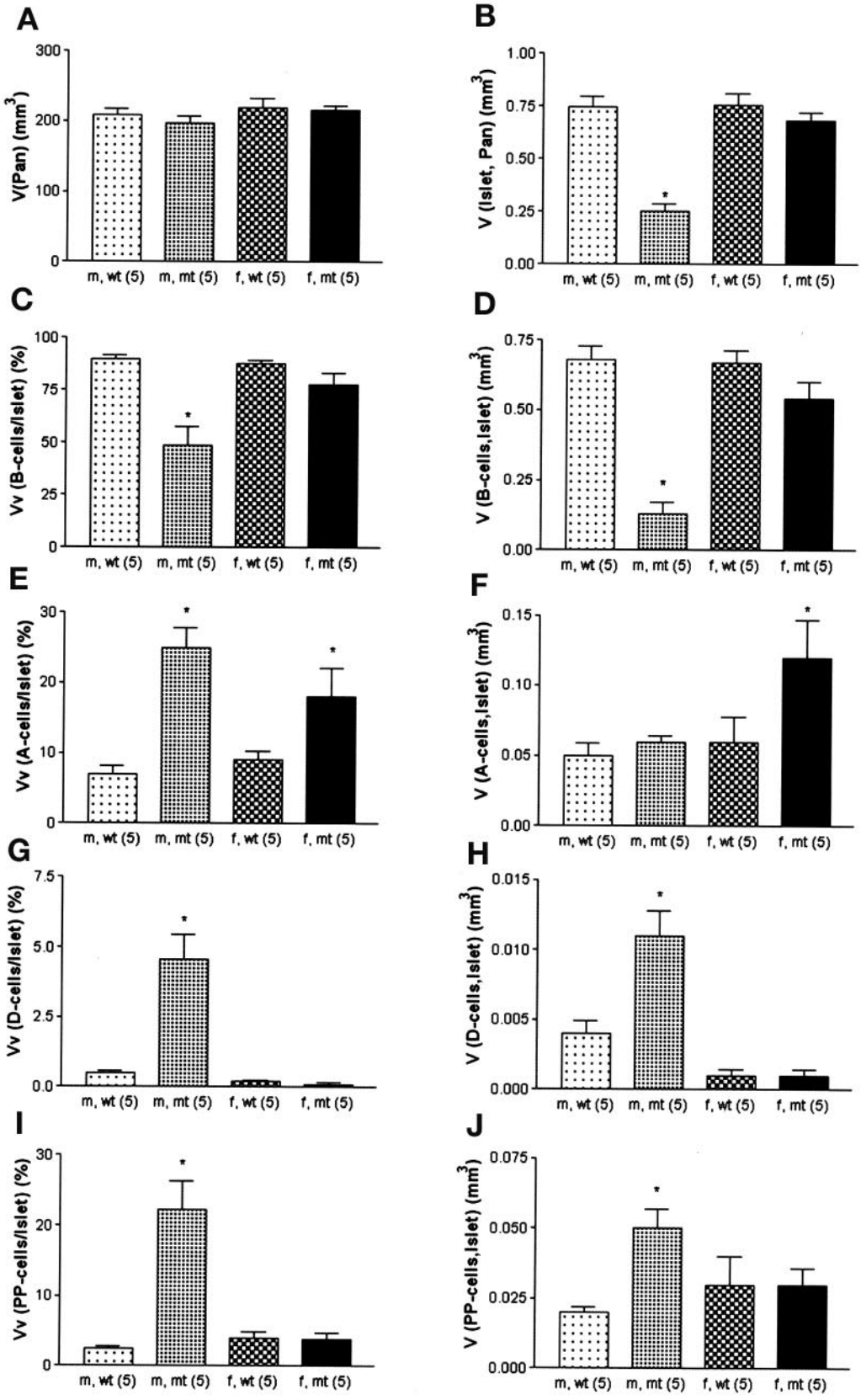

FIG. 6. Quantitative stereological investigations of the pancreas at 6 months of age. The pancreas volume (*A*) does not differ between groups. The total islet volume [$V_{(\text{Islet, Pan})}$] is significantly lower in male (m) mutants (mt) compared with male wild-type (wt) mice (*B*). The calculated volume density of β-cells in the islets [$Vv_{(\text{B-cells, Islet})}$; *C*] and the calculated total β-cell volume [$V_{(\text{B-cells, Islet})}$; *D*] is significantly lower in male mutant mice versus wild-type mice. The volume density of α-cells [$Vv_{(\text{A-cells, Islet})}$; *E*] is increased in mutant versus wild-type mice. The total α-cell volume [$V_{(\text{A-cells, Islet})}$; *F*] is increased in female (f) mutant versus wild-type mice. The volume density of δ-cells [$Vv_{(\text{D-cells, Islet})}$; *G*] and PP-cells [$Vv_{(\text{PP-cells, Islet})}$; *I*] and the total δ-cell [$V_{(\text{D-cells, Islet})}$; *H*] and PP-cell [$V_{(\text{PP-cells, Islet})}$; *J*] volumes are significantly higher in male mutant mice compared with wild-type mice. Data represent means and SE. *$P < 0.05$.

DISCUSSION

The present study shows that a point mutation at nucleotide position 1903 of *Ins2* causes severe diabetes in heterozygous Munich *Ins2*^{C95S} mutant mice. The strain was generated in the screen for dominant mutations of the Munich ENU mouse mutagenesis project. Establishment of the strain was carried out by repetitive breeding of diabetic heterozygous mutants to wild-type mice on the C3H genetic background for >10 generations. This led to the subsequent loss of additional phenotypically unapparent mutations caused by ENU from the Munich *Ins2*^{C95S} genome by segregation. The appearance of the diabetic phenotype was unaltered in the various generations, and N2 mice showed complete phenotypic penetrance of the mutation, thereby indicating that diabetes of Munich *Ins2*^{C95S} mutant mice is caused by the defined mutation revealed in the candidate gene analysis according to the results of linkage analysis (11).

The point mutation leads to the amino acid exchange C95S resulting in the loss of the A6-A11 intrachain disulfide bond. In vitro studies showed that the A6-A11 intrachain disulfide bond is of significant importance for the biologic activity of insulin. This mutant insulin retained ~60% of immunoactivity, and the conformation remained very similar to human insulin (12). The fasted and postprandial insulin levels of Munich *Ins2*^{C95S} mutant mice were indistinguishable from those of wild-type mice. However, first-phase insulin secretion was found to be diminished in heterozygous mutant mice and the HOMA β-cell index was significantly reduced. Therefore, Munich *Ins2*^{C95S} mice develop severe β-cell dysfunction. Homozygous Munich *Ins2*^{C95S} mutant mice show an even more pronounced diabetic phenotype and die within 2 months after weaning. Since *Ins2* knockout mice do not develop diabetes or hypoinsulinemia (13), the production of mutant insulin is thought to cause the β-cell dysfunction observed in Munich *Ins2*^{C95S} mutant mice by a dominant-negative mechanism. Several dominant-negative mechanisms may be postulated, such as downregulation of the synthesis of wild-type insulin, cross-linkage of mutant and wild-type proinsulin/insulin, and cytotoxicity by mutant insulin leading to β-cell loss (14). In type 2 diabetes, gluco- and lipotoxicity and increased insulin demand due to insulin resistance are thought to play a role in the development of β-cell dysfunction and death (15). As evidenced by insulin tolerance tests, Munich *Ins2*^{C95S} mutant male mice show a delayed response to exogenous insulin and the HOMA of insulin resistance index was increased. Therefore, an increased insulin demand could be responsible for the observed β-cell dysfunction in Munich *Ins2*^{C95S} mutant mice. However, insulin resistance was not observed at all time points examined, and calculation of the HOMA of insulin resistance index is not validated for mice; therefore, the results have to be interpreted carefully (6). Recent in vitro studies provide evidence that proinsulin lacking the intrachain disulfide bond may exhibit a disturbed formation of the other disulfide bonds, which leads to misfolding of the protein (16). Low-level and long-term misfolding of proteins in the endoplasmic reticulum is thought to lead to β-cell exhaustion and to chronic endoplasmic reticulum stress (17). Therefore, the accumulation of mutant proinsulin^{C95S} in the endoplasmic reticulum could lead to the induction of endoplasmic reticulum stress and thereby induce β-cell dysfunction and diabetes in the Munich *Ins2*^{C95S} mutant mouse. The Akita mouse is an *Ins2* mutant model on a C57BL/6N genetic background, which dominantly develops early-onset diabetes without insulitis or obesity (18). The animals exhibit a G→A transition at nucleotide position 1907 in exon 3 of *Ins2*, leading to the amino acid exchange C96Y, the disruption of the A7-B7 interchain disulfide bond, and the appearance of a severe defect in insulin secretion and hypoinsulinemia in heterozygous mutants. The C96Y mutant insulin is trapped in the endoplasmic reticulum and degraded intracellularly (19). In the Akita mouse, the accumulation of mutant insulin in β-cells is thought to be responsible for the delayed onset of diabetes rather than the initial lack of active insulin (14,20).

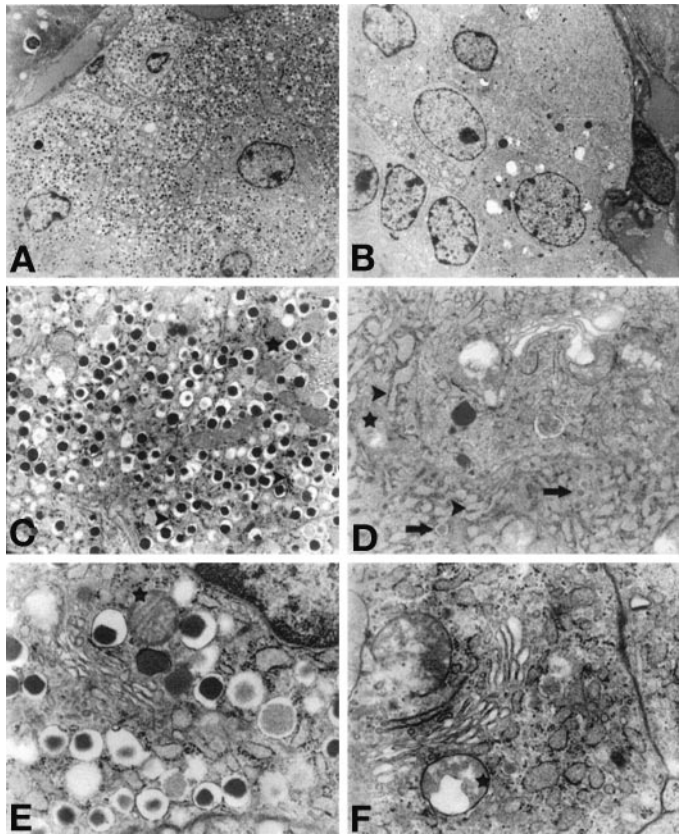

FIG. 7. Electron microscopy of β-cells of a C3H wild-type mouse (*A*, *C*, and *E*) and a representative heterozygous Munich *Ins2*^{C95S} mutant mouse (*B*, *D*, and *F*). There are very few small secretory insulin granules (arrows) in the β-cells of mutant mice, and the electron lucent halo between the core and the limiting membrane is narrow. The endoplasmic reticulum (arrow heads) of mutant mice is dilated, and mitochondria (asterisks) are swollen with disintegration of crests.

Pancreas weight was not altered, and both gross morphology and histologic appearance of the exocrine pancreas were inconspicuous in Munich *Ins2*^{C95S} mutant mice. The endocrine pancreas, however, showed striking light microscopic changes without insulitis. Immunohistochemistry revealed a disturbed islet cell composition accompanied by a changed distribution of endocrine cells in islets and severe reduction of the β-cell mass of male mutants. In female mutants, β-cell mass was not found to be reduced, which can explain the stable and milder diabetic phenotype, whereas glucose homeostasis in males rapidly deteriorates. This phenomenon could be explained by antidiabetic actions of 17β-estradiol (E2) in both humans and rodents. E2 is known for its effects on skeletal muscle, adipose tissue, liver, and pancreatic β-cell function and survival (21).

The slow accumulation of mutant proinsulin in the endoplasmic reticulum of Munich *Ins2*^{C95S} mutants would lead to disturbed endoplasmic reticulum function and endoplasmic reticulum stress, which could explain the severe β-cell loss of male Munich *Ins2*^{C95S} mutant mice. However, other mechanisms might also be responsible for the reduced β-cell viability, including oxidative stress due to insulin resistance and sustained elevation of cytosolic calcium concentrations due to overstimulation by high glucose levels (15,22). Heterozygous mutant Akita mice also show a significant decrease of the relative insulin-positive area, and homozygous Akita mice show an additional decrease of the relative islet area and an increase of the glucagon-positive area in the islets (18,23). In contrast to mice exhibiting a point mutation in the proinsulin gene, mice lacking the *Ins1* and/or *Ins2* gene show enlarged islets (13,24,25). This finding further underlines the dominant-negative phenotype of mice expressing mutant insulin.

The ultrastructure of the β-cells of Munich *Ins2*^{C95S} mutants was severely disrupted compared with wild-type mice. The typical insulin secretory granules, which appear in high numbers in wild-type mice and are characterized by an electron-dense core and a large electron lucent halo between the content and the limiting membrane, were almost lost in β-cells of mutant mice, and remaining granules appeared immature. Degranulation of β-cells is a well-known finding in long-term diabetes. Chronic exposure to high glucose levels impairs insulin production and leads to the depletion of insulin content (26). There were no signs of nuclear apoptosis of Munich *Ins2*^{C95S} mutant β-cells; however, it has been reported that β-cell death can occur without characteristic features of apoptosis (27), and nuclear changes are not required for programmed cell death (28,29). Damaged cells of Munich *Ins2*^{C95S} mutants showed extensive endoplasmic reticulum dilatation comparable with that described for enucleated cells undergoing cytoplasmic apoptosis (28,29). In the Akita mouse, no significant difference was observed in the number of apoptotic cells, despite exhaustive sectioning of all pancreatic islets (14). However, apoptosis is considered to be of significant importance for β-cell loss in Munich *Ins2* mutant mice, similar to the situation in Akita mice, as well as in human diabetes.

In contrast to Munich *Ins2*^{C95S} mutant mice, the amount of secretory granules of heterozygous Akita mice was comparable with wild-type mice. However, in homozygous Akita mouse mutants, the amount of granules was reported to be reduced and granules were smaller than those of wild-type mice (23). Similar to the Akita mouse (14,23,30), the endoplasmic reticulum of Munich *Ins2*^{C95S} mutant mice was noted to be distended, and mitochondria were enlarged and denatured. These morphologic changes are thought to reflect an impairment of the secretory pathway of Akita mouse β-cells (14). In Akita mouse islets, the transport efficiency of early secretory pathways was found to be reduced, and misfolded proinsulin 2 was thought to accumulate in the β-cells (14,19). However, recent in vitro studies showed that misfolded insulin 2 C96Y does not accumulate, and it was suggested that it is subjected to increased intracellular degradation (31). Studies in MIN6 cells, expressing the mutant *Ins2*^{C95S} gene in a tetracycline-responsive system, are currently under investigation to get more insight into the mechanisms of β-cell dysfunction and death, which occurrs in Munich *Ins2*^{C95S} mutant mice.

In this study, we present a novel mutant mouse model of early-onset diabetes without preceding obesity or insulitis. Mutant mice exhibit a reduction of the β-cell mass and severe ultrastructural changes of the β-cells and, therefore, represent an excellent tool for studying the mechanisms of β-cell dysfunction and death, as well as for therapeutic intervention studies.

ACKNOWLEDGMENTS

This work was supported by the Deutsche Forschungsgemeinschaft (Gk 1029 to N.H. and R.W.), the German Human Genome Project (DHGP to B.R. and M.K.), and the National Genome Research Network (NGFN). Additional funding was provided by the GSF.

We thank A. Siebert for excellent technical assistance.

REFERENCES

1. Wild S, Roglic G, Green A, Sicree R, King H: Global prevalence of diabetes: estimates for the year 2000 and projections for 2030. *Diabetes Care* 27:1047–1053, 2004
2. Mohr M, Klempt M, Rathkolb B, de Angelis MH, Wolf E, Aigner B: Hypercholesterolemia in ENU-induced mouse mutants. *J Lipid Res* 45: 2132–2137, 2004
3. Klaften M, Whetsell A, Webster J, Grewal R, Fedyk E, Einspanier R, Jennings J, Lirette R, Glenn K: Animal biotechnology: challenges and prospects. In *ACS Symposium Series 866.* Bhalgat MM, Ridley WP, Felsot AS, Seiber JN, Eds. Washington, DC, American Chemical Society, 2004, p. 83–99
4. Kemter E, Philipp U, Klose R, Kuiper H, Boelhauve M, Distl O, Wolf E, Leeb T: Molecular cloning, expression analysis and assignment of the porcine tumor necrosis factor superfamily member 10 gene (TNFSF10) to SSC13q34–>q36 by fluorescence in situ hybridization and radiation hybrid mapping. *Cytogenet Genome Res* 111:74–78, 2005
5. Herbach N, Goeke B, Schneider M, Hermanns W, Wolf E, Wanke R: Overexpression of a dominant negative GIP receptor in transgenic mice results in disturbed postnatal pancreatic islet and beta-cell development. *Regul Pept* 125:103–117, 2005
6. Wallace TM, Levy JC, Matthews DR: Use and abuse of HOMA modeling. *Diabetes Care* 27:1487–1495, 2004
7. Pamir N, Lynn FC, Buchan AM, Ehses J, Hinke SA, Pospisilik JA, Miyawaki K, Yamada Y, Seino Y, McIntosh CH, Pederson RA: Glucose-dependent insulinotropic polypeptide receptor null mice exhibit compensatory changes in the enteroinsular axis. *Am J Physiol Endocrinol Metab* 284:E931–E939, 2003
8. Wanke R, Weis S, Kluge D, Kahnt E, Schenck E, Brem G, Hermanns W: Morphometric evaluation of the pancreas of growth hormone-transgenic mice. *Acta Stereol* 13:3–8, 1994
9. Gundersen HJ, Bendtsen TF, Korbo L, Marcussen N, Moller A, Nielsen K, Nyengaard JR, Pakkenberg B, Sorensen FB, Vesterby A, et al.: Some new, simple and efficient stereological methods and their use in pathological research and diagnosis. *APMIS* 96:379–394, 1988
10. Sachs L: *Angewandte Statistik.* Berlin, Springer Verlag, 2004
11. Keays DA, Clark TG, Flint J: Estimating the number of coding mutations in genotypic- and phenotypic-driven N-ethyl-N-nitrosourea (ENU) screens. *Mamm Genome* 17:230–238, 2006
12. Dai Y, Tang JG: Characteristic, activity and conformational studies of [A6-Ser, A11-Ser]-insulin. *Biochim Biophys Acta* 1296:63–68, 1996
13. Leroux L, Desbois P, Lamotte L, Duvillie B, Cordonnier N, Jackerott M, Jami J, Bucchini D, Joshi RL: Compensatory responses in mice carrying a null mutation for Ins1 or Ins2. *Diabetes* 50 (Suppl. 1):S150–S153, 2001
14. Izumi T, Yokota-Hashimoto H, Zhao S, Wang J, Halban PA, Takeuchi T: Dominant negative pathogenesis by mutant proinsulin in the Akita diabetic mouse. *Diabetes* 52:409–416, 2003
15. Cnop M, Welsh N, Jonas JC, Jorns A, Lenzen S, Eizirik DL: Mechanisms of pancreatic β-cell death in type 1 and type 2 diabetes: many differences, few similarities. *Diabetes* 54 (Suppl. 2):S97–S107, 2005
16. Liu M, Li Y, Cavener D, Arvan P: Proinsulin disulfide maturation and misfolding in the endoplasmic reticulum. *J Biol Chem* 280:13209–13212, 2005
17. Oyadomari S, Araki E, Mori M: Endoplasmic reticulum stress-mediated apoptosis in pancreatic beta-cells. *Apoptosis* 7:335–345, 2002
18. Yoshioka M, Kayo T, Ikeda T, Koizumi A: A novel locus, Mody4, distal to

D7Mit189 on chromosome 7 determines early-onset NIDDM in nonobese C57BL/6 (Akita) mutant mice. *Diabetes* 46:887–894, 1997
19. Wang J, Takeuchi T, Tanaka S, Kubo SK, Kayo T, Lu D, Takata K, Koizumi A, Izumi T: A mutation in the insulin 2 gene induces diabetes with severe pancreatic beta-cell dysfunction in the Mody mouse. *J Clin Invest* 103:27–37, 1999
20. Oyadomari S, Koizumi A, Takeda K, Gotoh T, Akira S, Araki E, Mori M: Targeted disruption of the Chop gene delays endoplasmic reticulum stress-mediated diabetes. *J Clin Invest* 109:525–532, 2002
21. Louet JF, LeMay C, Mauvais-Jarvis F: Antidiabetic actions of estrogen: insight from human and genetic mouse models. *Curr Atheroscler Rep* 6:180–185, 2004
22. Grill V, Bjorklund A: Overstimulation and β-cell function. *Diabetes* 50 (Suppl. 1):S122–S124, 2001
23. Kayo T, Koizumi A: Mapping of murine diabetogenic gene mody on chromosome 7 at D7Mit258 and its involvement in pancreatic islet and beta cell development during the perinatal period. *J Clin Invest* 101:2112–2118, 1998
24. Duvillie B, Cordonnier N, Deltour L, Dandoy-Dron F, Itier JM, Monthioux E, Jami J, Joshi RL, Bucchini D: Phenotypic alterations in insulin-deficient mutant mice. *Proc Natl Acad Sci U S A* 94:5137–5140, 1997
25. Duvillie B, Currie C, Chrones T, Bucchini D, Jami J, Joshi RL, Hill DJ: Increased islet cell proliferation, decreased apoptosis, and greater vascularization leading to beta-cell hyperplasia in mutant mice lacking insulin. *Endocrinology* 143:1530–1537, 2002
26. Kaiser N, Leibowitz G, Nesher R: Glucotoxicity and beta-cell failure in type 2 diabetes mellitus. *J Pediatr Endocrinol Metab* 16:5–22, 2003
27. Herrera PL, Harlan DM, Vassalli P: A mouse CD8 T cell-mediated acute autoimmune diabetes independent of the perforin and Fas cytotoxic pathways: possible role of membrane TNF. *Proc Natl Acad Sci U S A* 97:279–284, 2000
28. Schulze-Osthoff K, Krammer PH, Droge W: Divergent signalling via APO-1/Fas and the TNF receptor, two homologous molecules involved in physiological cell death. *EMBO J* 13:4587–4596, 1994
29. Jacobson MD, Burne JF, Raff MC: Programmed cell death and Bcl-2 protection in the absence of a nucleus. *EMBO J* 13:1899–1910, 1994
30. Zuber C, Fan JY, Guhl B, Roth J: Misfolded proinsulin accumulates in expanded pre-Golgi intermediates and endoplasmic reticulum subdomains in pancreatic beta cells of Akita mice. *FASEB J* 18:917–919, 2004
31. Allen JR, Nguyen LX, Sargent KE, Lipson KL, Hackett A, Urano F: High endoplasmic reticulum stress in beta-cells stimulates intracellular degradation of misfolded insulin. *Biochem Biophys Res Commun* 324:166–170, 2004